

# Chromatic Losses in Natural Scenes with Viewing Distance

Raúl Luzón-González,<sup>1\*</sup> Sérgio M. C. Nascimento,<sup>2</sup>  
Osamu Masuda,<sup>2</sup> Javier Romero<sup>1</sup>

<sup>1</sup>Optics Department, University of Granada, Campus Universitario Fuentenueva, Fuentenueva s/n, 18071 Granada, Spain

<sup>2</sup>Department of Physics, Gualtar Campus, University of Minho, 4710-057 Braga, Portugal

Received 26 October 2012; revised 19 January 2013; accepted 7 February 2013

*Scattering and absorption in the atmosphere influence the colors of objects and can dramatically affect the way a landscape is perceived. We estimated, computationally, the chromatic losses in natural scenes as a function of the viewing distance for several atmospheric conditions. The study was based on models of real atmospheric scattering and absorption applied to hyperspectral data from natural images. It was found that exponential models could describe well the reduction in the number of perceived colors as a function of the viewing distance and the relationship between the coefficient reflecting the sum of the scattering and absorption effects and the viewing distance for a 50% reduction in colors. These results provide simple models to estimate the chromatic losses with viewing distance and can be used in applications of atmospheric optics concerned with visual simulations.* © 2013 Wiley Periodicals, Inc. *Col Res Appl*, 39, 341–346, 2014; Published Online 12 April 2013 in Wiley Online Library (wileyonlinelibrary.com). DOI 10.1002/col.21812

*Key words:* color; visibility and imaging; atmospheric optics; atmospheric scattering

## INTRODUCTION

When we observe the objects of a natural scene at a distance, their original colors, that is, those observed when seen very near, are modified by the scattering and absorption of light in the atmosphere.<sup>1,2</sup> The light reflected by the objects suffers attenuation which can be spectrally selective, due to scattering and absorption phenomena

along the trajectory from the objects to the observer. Also, scattered light in the atmosphere by particles out of this trajectory is added to the direct light. This is the component of the light received by the observer called airlight.<sup>2</sup> As a consequence of these two phenomena, the objects appear whitish, with less-saturated colors, and in some occasions, with a tendency to bluish. These effects and others atmospheric optical phenomena have been explored by artists for centuries.<sup>3</sup> When the size of the particles is less than 10% of the wavelength of the incident light, the scattering process can be explained according to the Rayleigh theory, which is strongly dependent on the wavelength. For particle sizes of about the same size or larger than 10% of the wavelength, such as those in water vapor, the scattering process is explained using the Mie theory, according to which the dependence between light scattering and wavelength decreases.<sup>2</sup> These effects influence the final color of the objects seen by an observer or detected by a camera and both a change in the color distributions and a reduction in the number of colors are expected with increasing distance.

Hendley and Hetch<sup>4</sup> made a first psychophysical evaluation of the color of the objects when viewed at a certain distance. They took notice of the lost in saturation and excitation purity for objects observed at a long distance. This decrease in the chromaticity of the objects with the distance in terms of the colorfulness has been also reported by Henry *et al.*<sup>5</sup> Recently,<sup>6</sup> we have computed the chromaticity coordinates of a set of opaque objects when observed from 0 km to  $\infty$ , according to a dichromatic model of scattering in the atmosphere.<sup>7</sup> We have shown that the evolution of the chromaticity coordinates of the object along the chromaticity diagram goes from its original colors, when viewed at 0 distance, to the chromaticity of the horizon when the object is viewed at very long distance. This evolution means a lost in the

\*Correspondence to: Raúl Luzón-González (e-mail: raul@ugr.es).

Contract grant sponsor: Junta de Andalucía, Spain; contract grant number: P07.TIC.02642.

saturation of the objects' color and a certain change in the hue of the objects to blue which depends on the atmospheric conditions.

The purpose of this work was to estimate, computationally, the extent of the chromatic losses in natural scenes as a function of the viewing distance for several atmospheric conditions and to investigate the extent to which the losses can be described by simple quantitative models. Such models can be useful in applications of atmospheric optics such as in computer simulations of the outdoors scenes viewed through fog<sup>8</sup> and in visual pilot training simulators.<sup>9</sup>

We used a dichromatic model of the atmosphere that has been introduced to perform algorithms to recover original images from the degradation introduced by scattering and absorption.<sup>7,10–13</sup> As the losses due to degradation of spatial resolution are trivial they were not considered here.<sup>14</sup>

## METHOD

Assuming the dichromatic atmospheric scattering model,<sup>7</sup> the spectral radiance which exhibits an object with a spectral reflectance  $\rho(\lambda)$ , when it is observed at a certain distance, has two components, one induced by direct light coming from the object toward the observer and the other by added light in the observer's cone of vision due to atmospheric scattering or airlight. Thus, the object's spectral radiance observed at a distance  $d$  can be expressed as

$$L(\lambda, d) = L_0(\lambda) \exp(-\beta(\lambda)d) + L_\infty(\lambda)(1 - \exp(-\beta(\lambda)d)) \quad (1)$$

where  $L_0(\lambda)$  is the object's spectral radiance at zero distance,  $\beta(\lambda)$  is the extinction coefficient in the atmosphere, and  $L_\infty(\lambda)$  is the spectral radiance of the airlight for an infinity distance, in practice the radiance of the horizon. The first term of Eq. (1) represents attenuated direct light whilst the second one represents the airlight. We assume a homogeneous atmosphere, that is,  $\beta(\lambda)$  is taken to be the same through the trajectory from the object to the observer and that the spectral illuminant is constant through the whole scene. In cloudy days Eq. (1) could be expressed as<sup>7</sup>

$$L(\lambda, d) = L_\infty(\lambda)\rho(\lambda)\exp(-\beta(\lambda)d) + L_\infty(\lambda)(1 - \exp(-\beta(\lambda)d)) \quad (2)$$

where  $L_\infty(\lambda)$  can be substituted by the spectral radiance of a perfect white object in the scene.<sup>15</sup>

In the computations, we used scattering and absorption coefficients measured in five days covering a wide range of atmospheric conditions, from very clean atmosphere to hazy atmosphere, corresponding to a range of extinction coefficients between 50 to 150  $\text{Mm}^{-1}$  in the spectral range from 400 to 720 nm.

The extinction coefficient,  $\beta(\lambda)$ , is the sum of the scattering and the absorption coefficients. The scattering coefficient was measured at three wavelengths (450, 550, and 700 nm) and extrapolated to the range between (400 and 720 nm) using the expression:

$$\beta(\lambda) \propto \frac{1}{\lambda^u} \quad (3)$$

where the parameter  $u$  is related with the amount and type of aerosols present in the atmosphere.<sup>2</sup> More details about the characteristics of the atmospheric conditions can be found in the work Romero *et al.*<sup>6</sup> In the visible range, the absorption coefficient was taken to be constant and measured at 670 nm.<sup>16</sup>

The effects of the different extinction coefficients and distances were simulated using hyperspectral data from 17 rural scenes of non-cultivated areas, containing rocks, trees, flowers, grass, foliage, and earth, and 21 urban environments containing buildings. The hyperspectral data were obtained with a hyperspectral imaging system consisting of digital camera with a spatial resolution of  $1344 \times 1024$  pixels (Hamamatsu, model C4742-95-12ER, Hamamatsu Photonics K. K., Japan), and a fast tunable liquid-crystal filter (Varispec, model VS-VIS2-10-HC-35-SQ, Cambridge Research & Instrumentation, MA). The tunable filter was mounted in front of a lens with a 75 mm focal length. The viewing angle of the system was about  $6^\circ$  and its spatial resolution was comparable to that of the human eye. The images were acquired in the range 400–720 nm in 10 nm steps. Hyperspectral data were calibrated using the spectrum of the light reflected from a gray surface present in the scene measure with a telespectroradiometer (SpectraColourimeter, PR-650, PhotoResearch, Chatsworth, CA) just after image acquisition. The data necessary for the computations carried out here were the spectral reflectance and the spectral radiance from a perfect white object of the scene. The spectrum from the gray reference surface was used to obtain the spectral radiance from a perfect white object and to normalize for the illumination of the scene and therefore to obtain an estimate of the spectral reflectance of each pixel (see the work of Foster and Amano<sup>15</sup> for details about the imaging technique and Linhares *et al.*<sup>17</sup> for pictures of the scenes). For each pixel on an image, the corresponding spectral radiance was estimated according to Eq. (2), considering a distance  $d$  and an extinction coefficient  $\beta$ . The illuminant used for the simulations was the one recovered from the scene.<sup>15</sup> As a white reference, we have employed a perfect white patch ( $\rho(\lambda) = 1$ ) at every distance. We have employed the CIE 1931 Standard Colorimetric Observer.<sup>18</sup> The CIELAB<sup>18</sup> color coordinates were computed and in this way we obtain the color gamut of the scene in such conditions. The number of discernible colors was estimated by segmenting the CIELAB color volume into unitary cubes and by counting the number of non-empty cubes, a methodology that produces a reasonable estimate.<sup>17,19</sup> Next, we studied the decrease in the number of discernible colors of the scenes with the distance of observation, at certain atmospheric conditions.

## RESULTS

Figure 1 shows the results of the computations for two scenes, one for an urban scene and the other for a rural scene with two different beta parameters. The first and

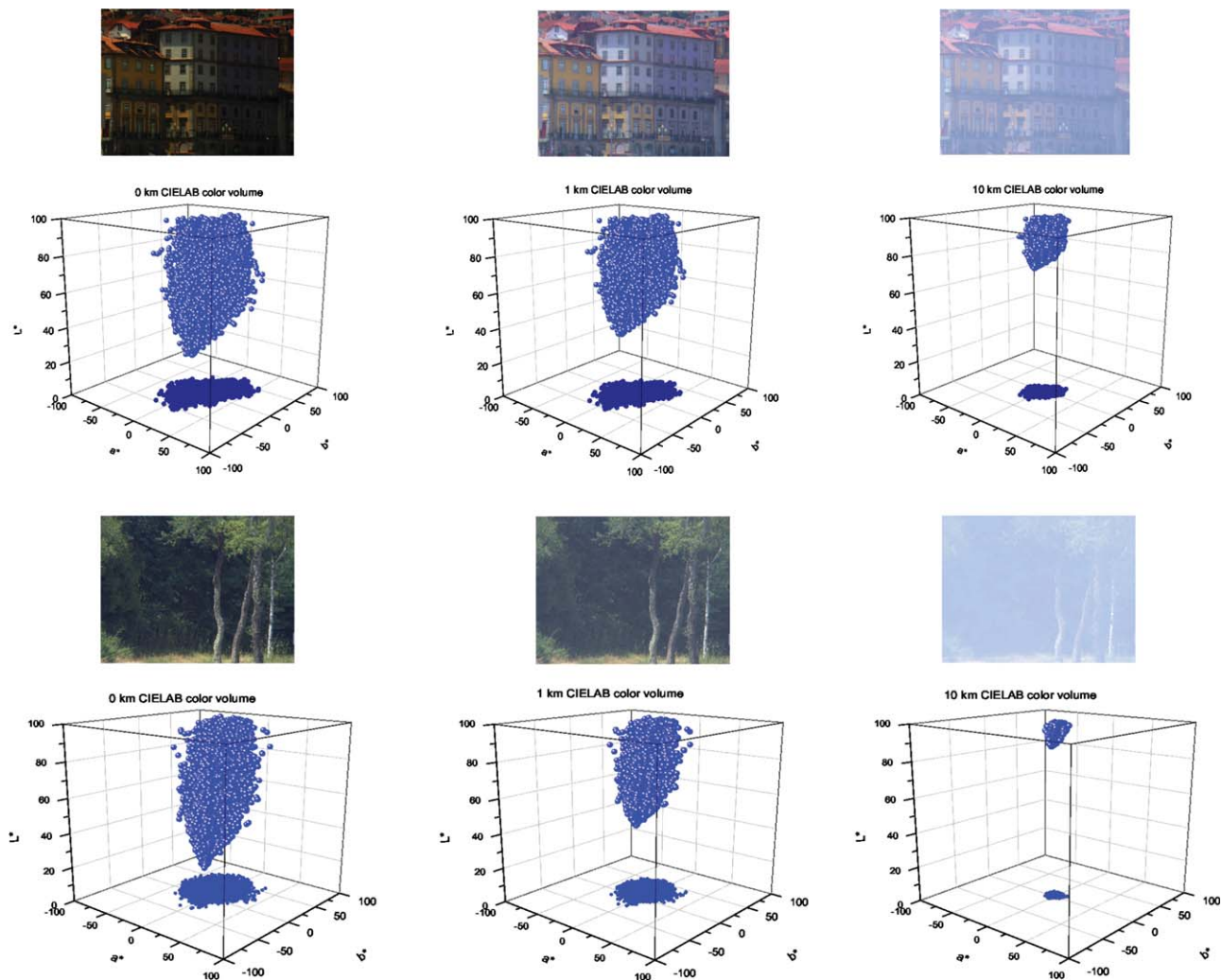


FIG. 1. First and third row corresponds to a RGB sample images (electronic version) obtained from the hyperspectral data at three distances (0 km, 1 km, and 10 km). The first row corresponds to an urban scene in a clear day ( $\beta = 60.3 \text{ Mm}^{-1}$ ), and the third row corresponds to a rural scene in a hazy day ( $\beta = 125.2 \text{ Mm}^{-1}$ ). The second and fourth rows corresponds to the CIELAB coordinates for each scene at three distances.

third rows corresponds to the RGB representation obtained from the hyperspectral images (electronic version), used here for representational purposes. The first column correspond to the original scene (observation distance at 0 km), the second one is for an observation distance of 1 km, and the third one for 10 km. The simulations were run keeping the scene geometry unchanged but increasing the simulated distance to the observation point. The second and fourth rows correspond to the CIELAB coordinates for each scene and for each distance. These plots show a reduction in the color gamut of the objects in the scene as the distance increases. As we previously showed in Romero *et al.*<sup>6</sup> the chromaticity of the objects tends to the color coordinates of the horizon as the observation distance increases. This can be deduced from Eq. (2). Also, as a consequence of the spectral dependency of the airlight term, introduced by the extinction coefficient, this tendency is faster for the objects with hue different than blue. Then, the typical shift of the objects' color toward a bluish hue was found.

The airlight component adds environmental light in the observer's field of view and introduces a desaturation in the color of the objects as the distance of observation increases. Then, the  $(a^*, b^*)$  color coordinate gamut are compacted yielding to a chromatic reduction when the distance increases. The lightness component ( $L^*$  coordinate) drifts to the limiting value of 100 due to the effect of the airlight term. As a consequence of the compression in the chromatic components ( $a^*, b^*$  coordinates) and the increase in lightness component ( $L^*$  coordinate), objects appears less saturated and whitish. In the limit, for an infinite distance, the color information of the objects is lost, as predicted by Eq. (2), and only environmental scattering light will arrive at the observer. Thus, the visibility of the objects in the scene shrinks increasingly with the scene distance. This reduction in the color gamut of the scene's objects was found for all scenes and for all atmospheric conditions.

We have evaluated numerically this reduction in the color gamut of the scenes by the estimation of the

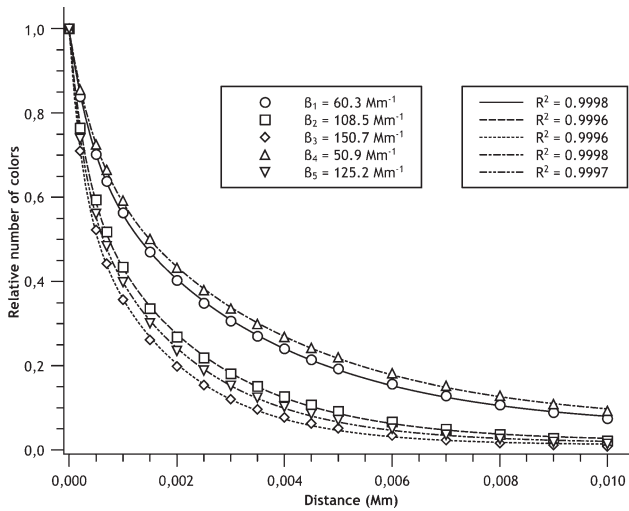


FIG. 2. Decline of the discernible colors averaged for all scenes as a function of the distance for five extinction coefficients. The lines correspond to an exponential fit of the form  $y_0 + a_1 \exp(-x/t_1) + a_2 \exp(-x/t_2)$ , with a goodness of fit showed in the plot, where  $y_0$ ,  $a_1$ ,  $a_2$ ,  $t_1$ , and  $t_2$  are the parameters.

number of discernible colors in each scene and atmospheric conditions, Fig. 2. The results are normalized to the value for 0 km of observation distance. We found that the number of discernible colors for all images in the database and for all atmospheric conditions considered is reduced exponentially as the distance increases. Figure 2 shows the reduction in the number of discernible colors for five different atmospheric conditions for all scenes in the database. For higher extinction coefficients (i.e., turbid atmosphere), the number of discernible colors is lower than the obtained for lower extinction coefficients (i.e., clean atmosphere). The fit of a double exponential to the data is shown in Fig. 2.

The term due to attenuation in the Eq. (2), first addend, is plotted separately in Fig. 3. The attenuation component

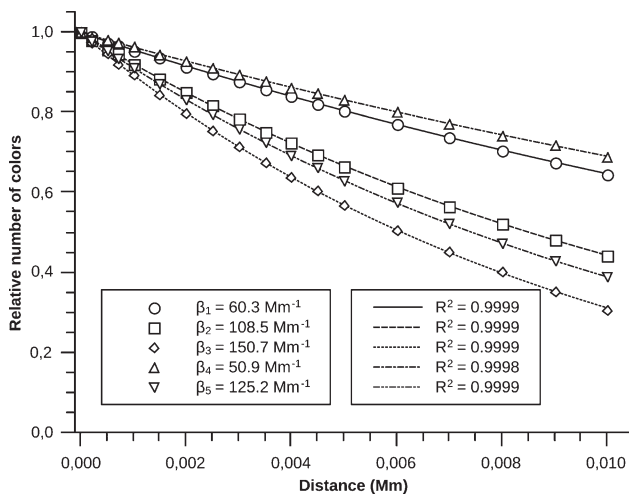


FIG. 3. Reduction of the discernible colors for the attenuation term. In this case the lines correspond to an exponential fit of the form  $y_0 + a \exp(-x/t)$ , with a goodness of fit showed in the plot, where  $y_0$ ,  $a$ , and  $t$  are the parameters.

TABLE I. Decay parameters ( $t_1$  and  $t_2$ ) of the exponential fit for five extinction coefficients ( $\beta$ ).

Extinction coefficient ( $\text{Mm}^{-1}$ )	$t_1$ ( $10^{-3}$ )	$t_2$ ( $10^{-3}$ )
$\beta_1 = 60.3$	0.4	3.2
$\beta_2 = 108.5$	0.3	2.2
$\beta_3 = 150.7$	0.2	1.7
$\beta_4 = 50.9$	0.5	3.5
$\beta_5 = 125.2$	0.3	2.0

The fit shows that there are two components involved in the reduction of discernible colors as distance increase, one slower (related with the attenuation component,  $t_1$ ) and one faster (related with the airlight component,  $t_2$ ).

introduces a smooth reduction in the number of discernible colors. This attenuation term was adjusted to a single exponential fit with a high goodness of fit as it is shown in the plot. When Figs. 2 and 3 are compared it can be deduced that the airlight term influences in a higher degree the reduction in the number of discernible colors, especially for short distances. Table I shows the decay parameters obtained in the fits. The small one is related to the attenuation component and the larger one to the airlight component. The fast decrease of the number of colors from 0 to 4 km is mainly due to the airlight term in Eq. (2). For instance, at 2 km the total number of discernible colors is approximately between 20 and 43% of the original gamut, which is a reduction between 80 and 57% approximately, depending on the atmospheric conditions. In this case, the reduction due to attenuation is around 20% for the higher extinction coefficient. The reduction due to the attenuation term falls between 25 and 70% at 10 km. We can conclude that the principal factor responsible for the reduction in the color gamut of the scenes with distance is the airlight. Nevertheless, in some cases the attenuation term can be responsible for the total reduction in the number of colors at long distances at higher extinctions coefficients.

Figure 4 represents the extinction coefficient as a function of the distance for which the number of discernible colors falls by half. The red line (electronic version) represents an exponential fit with a goodness of fit value of 0.9917. The quality of this fit suggests that an exponential model can be used to estimate the reduction in the number of discernible colors in a specific scene as a function of the atmospheric conditions, independent of the color gamut of the scene.

The study was generalized to the optimal colours<sup>18</sup> which are object colors having the maximum saturation at a given lightness. Figure 5 represents a comparison between the volume enclosed by the optimal colors,<sup>20,21</sup> and the color volumes averaged for all the scenes and for all atmospheric conditions considered. The computations of the volume of the solid were carried out as described in the work by Masuda and Nascimento.<sup>22</sup> The reduction in theoretical volume follows a similar behavior to the one obtained with the data from the natural scenes, but

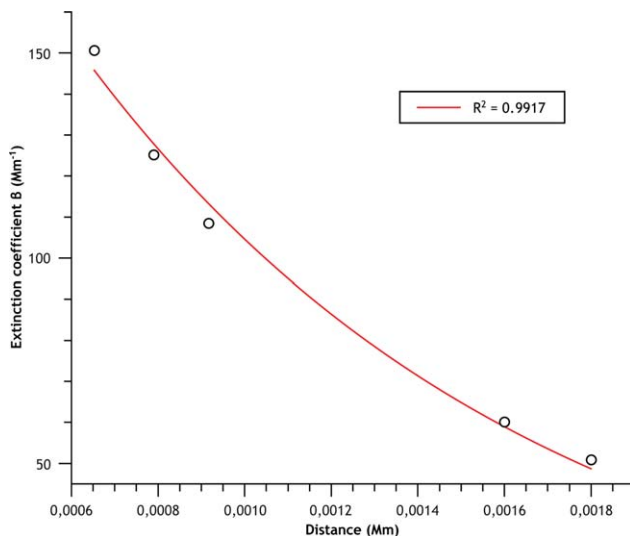


FIG. 4. Extinction coefficient as a function of the distance where the number of discernible colors falls by half. The red line (electronic version) correspond to an exponential fit of the form  $a \exp(-x/t)$ , with a goodness of fit of 0.9917, where  $a$  and  $t$  are the parameters.

with faster decay. This may be explained by the fact that natural colors occupy only a fraction of the theoretical limits defined by optimal colours<sup>17</sup> and by the non-uniformities of the CIELAB color space near the limits.<sup>23,24</sup>

## CONCLUSION

In this work, we used CIELAB color space and assumed that the metric is such that Euclidian distances between colors are at 1:1 relationship to perceptual differences. However, the nonuniformities of this color space are well documented, especially close to the locus of spectral colours.<sup>23,24</sup> On the other hand, the influence of the spatial structure of the images on color perception and discrimination was not considered. As the estimates obtained here are relative rather than absolute these effects are minimized. In addition, the colors of the natural scenes, both of urban and rural environments, have a limited gamut and their colors rarely are close to the chromatic extremes where the CIELAB space is less uniform.<sup>17</sup>

We found that the reduction in the number of discernible colors with the distance of observation can be well described by an exponential decay with two components. A fast component determined by the airlight effect and a slow component determined by the attenuation effect. Also, we have shown that an exponential model describes the relationship between the extinction coefficient and the distance for which the reduction in the number of colors is halved.

The results of this work provide a simple way to estimate the color gamut reduction with distance in real scenes for different atmospheric conditions and can be useful as a first step in application of atmospheric optics such as color simulation of surfaces viewed through mist and in daylight pilot training simulators. These results

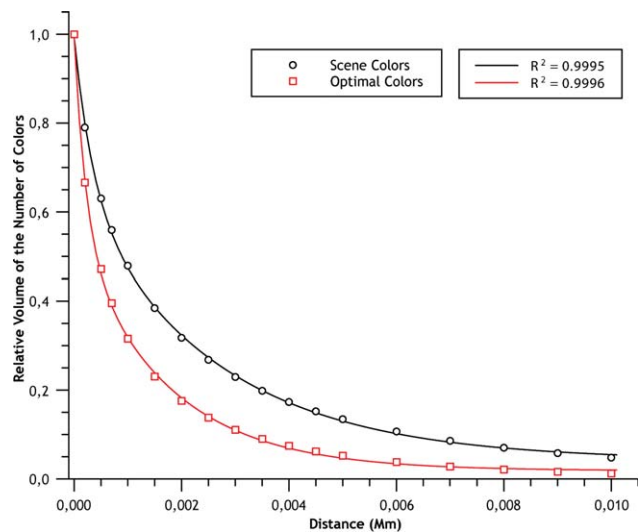


FIG. 5. Comparison between the speed reduction in the relative volumes of the objects colors in the scene (black round points) and the corresponding optimal colors (red square points, electronic version) as a function of the distance. The lines corresponds to an exponential fit of the form  $y_0 + a_1 \exp(-x/t_1) + a_2 \exp(-x/t_2)$ , with a goodness of fit showed in the plot, where  $y_0$ ,  $a_1$ ,  $a_2$ ,  $t_1$ , and  $t_2$  are the parameters.

must include some model in order to be useful to simulate the human perception through mist or haze. There are several works that treat the study of transparency perception<sup>5,8</sup> but a whole quantitative model needs to be developed that could predict quantitatively the effects of semi-transparent layers and the color gamut reduction as a function of the distance and the atmospheric weather conditions.

## ACKNOWLEDGMENTS

Authors thank professors Juan Luis Nieves and Javier Hernández Andrés at the University of Granada for their helpful comments.

1. Minnaert M. The Nature of Light and Colour in the Open Air. New York: Dover Publications, 1954.
2. McCartney EJ. Optics of the Atmosphere, Scattering by Molecules and Particles. New York: Wiley, 1976.
3. Gedzelman SD. Atmospheric optics in art. Appl Opt 1991;30:3514–3522.
4. Hendley CD, Hecht S. The colours of natural objects and terrains, and their relation to visual colour deficiency. J Opt Soc Am 1949;39:870–873.
5. Henry RC, Mahadey S, Urquijo S, Chitwood D. Colour perception through atmospheric haze. J Opt Soc Am A 2000;17:831–885.
6. Romero J, Luzón-González R, Nieves JL, Hernández-Andrés J. Colour changes in objects in natural scenes as a function of observation distance and weather conditions. Appl Opt 2011;50:F112–F120.
7. Narasimhan SG, Nayar SK. Vision and the atmosphere. Int J Comput Vis 2002;48:233–254.
8. Hagedorn J, D'Zmura M. Colour appearance of surfaces viewed through fog. Perception 2000;29:1169–1184.
9. Willis PJ. Visual simulation of atmospheric haze. Comput Graphics Forum 1987;6:35–41.

10. Oakley JP, Satherley BL. Improving image quality in poor visibility conditions using a physical model for contrast degradation. *IEEE Trans Image Process* 1998;7:167–179.
11. Narasimhan SG, Nayar SK. Chromatic framework for vision in bad weather. *Proceedings of IEEE Conference on Computer Vision and Pattern Recognition*, Hilton Head Island, South Carolina, 2000; p 598–605.
12. Narasimhan SG, Nayar SK. Contrast restoration of weather degraded images. *IEEE Trans Pattern Anal Mach Intell* 2003;25:713–724.
13. Tan KK, Oakley JP. Physics based approach to colour image enhancement poor visibility conditions. *J Opt Soc Am A* 2001;18:2460–2467.
14. Treibitz T, Schechner YY. Recovery limits in pointwise degradation. *IEEE International Conference on Computational Photography*, New York, 2009. p 1–8.
15. Foster DH, Amano K. Frequency of metamerism in natural scenes. *J Opt Soc Am A* 2006;23:2359–2372.
16. Lenoble J. *Atmospheric Radiative Transfer*. Hampton, VA: A Deepak Publishing; 1993.
17. Linhares JMM, Pinto PD, Nascimento SMC. The number of discernible colours in natural scenes. *J Opt Soc Am A* 2008;25:2918–2924.
18. Wyszecki W, Stiles WS. *Colour science, concepts and methods, quantitative data and formulae*. New York: Wiley, 1982.
19. Pointer MR, Attridge GG. The number of discernible colours. *Colour Res Appl* 1998;23:52–54.
20. MacAdam DL. Maximum visual efficiency of coloured materials. *J Opt Soc Am* 1935;25:361–367.
21. MacAdam DL. The theory of the maximum visual efficiency of coloured materials. *J Opt Soc Am* 1935;25:249–252.
22. Masuda O, Nascimento SMC. Lighting spectrum to maximize colourfulness. *Opt Lett* 2012;37:407–409.
23. Luo MR, Rigg B. Chromaticity-discrimination ellipses for surface colours. *Color Res Appl* 1986;11:25–42.
24. Melgosa M, Huertas R, Berns RS. Relative significance of the terms in the CIEDE2000 and CIE94 colour-difference formulas. *J Opt Soc Am A* 2004;21:2269–2275.

## BOOK REVIEWS

**Value Metrics for Better Lighting.** By Mark S. Rea, Bellingham, WA: SPIE Press, 2013, ISBN 978-0-8194-9322-4, 114 pp. \$40.00.

Professor Rea’s work, *Value Metrics for Better Lighting*, discusses the fundamental quantities used in illuminating engineering. It deals, in five chapters and seven appendices, with the measurement of matter, new metric concepts for added value in lighting, and the concept of unified illuminance. The book was written to celebrate the 25th anniversary of founding the Lighting Research Center of Rensselaer Polytechnic Institute.

With this book, it was the intention of Professor Rea to call attention to the fact that the value of lighting is a quotient of its benefits and cost, and that the benefits must be better evaluated to get to the real value of lighting. It is not enough to deal only with the costs, and think that value of lighting can simply be increased by lowering its cost.

The book starts with a very clear description of the fundamental quantities of light (only a minor deficiency is that it still uses the unit “nit,” which has been depreciated for some time now). Otherwise, one finds here a very clear description when  $V(\lambda)$  should be used, and when another spectral luminous efficiency function would be better. A subsection deals in this chapter with color, color appearance, and color matching, and the fundamental concept in colorimetry. Rea’s attempt to keep the description simple leads to a vague differentiation between two dimensional chromaticity and three-dimensional color (later in the book several times one finds the expressions chromaticity and “color” put into quotation marks, as synonyms). This reviewer is of the opinion that for a newcomer into lighting and colorimetry one short and clear distinction would make it easier to understand the terminology. This applies also to the

explanation of correlated color temperature, where naturally in the  $x, y$  diagram the “shortest lines” from the chromaticity of the test source to the Planck-line are not the shortest. A clearer description of the two branches of color rendering—as used today—that is, of color fidelity and color preference would have been appreciated by the reviewer (but this is certainly still a question that divides the experts dealing with color rendering).

The next chapter deals with the added value one would get with metrics beyond  $\text{lm/W}$  or  $\text{lm/m}^2$ . Mesopic vision is introduced with its simple metric based on visual performance, now getting global acceptance as CIE Publ. 191. To avoid unnecessary hopes, a few sentences about further investigation that are needed before this system can be introduced in street-lighting design would have been appreciated.

In the subsection on brightness, a very comprehensive description of experiments performed at LRC can be found, here one misses a comparison of the LRC results with other results, for example, those of the CIE Publ. 200 “CIE Supplementary System of Photometry.”

An additional subsection discussed the influence of optical radiation on the circadian rhythm of the human body (from the formulation you can already feel that the reviewer is not happy with the term “circadian light”). The group at LRC conducted extensive research in this field, and one gets an excellent overview on their results in this part of the book.

The subsection “beyond of color rendering and correlated color temperature” discusses some debatable questions. It is really an ethical question whether a lighting designer should install “food-display” lamps that enhance chroma (and as Prof. Rea correctly mentions “obscure” the real color of meat). A more direct guidance as to where color preference

(continued on page 398)